IL NUOVO CIMENTO Vol. 29 C, N. 2 Marzo-Aprile 2006
DOI 10.1393/ncc/i2005-10208-0

Non-invasive neutron diffraction analysis of marbles from the "Edificio con Tre Esedre" in Villa Adriana(*)

A. Filabozzi(1)(2), A. Pietropaolo(2)(1), C. Andreani(1)(2), M. P. De Pascale(1), G. Gorini(3), W. Kockelmann(4) and L. C. Chapon(4)

(1) *Università di Roma "Tor Vergata" - 00133 Rome, Italy*
(2) *CNR-INFM - Rome, Italy*
(3) *Università di Milano-Bicocca and CNR-INFM - 20126 Milan, Italy*
(4) *ISIS Facility, Rutherford Appleton Laboratory - Chilton, OX11 0QX, UK*

(ricevuto il 9 Dicembre 2005; revisionato il 21 Marzo 2006; approvato il 22 Marzo 2006)

Summary. — Roman marble fragments from the Villa Adriana at Tivoli (Rome) have been characterised by neutron diffraction. This study aimed at distinguishing between different marble types on the basis of the mineral phase compositions and the crystallographic textures. It is demonstrated that on a multi-detector time-of-flight neutron diffractometer a quantitative bulk texture analysis can be performed on a stationary marble sample in a matter of minutes. This potentially allows investigating large sample series or bulky, intact marble objects in a completely non-destructive manner. The texture information, along with other structure details, can be used as characterising feature to address questions of attribution and restoration of archaeological marble objects.

PACS 61.12.-q – Neutron diffraction and scattering.
PACS 81.70.-q – Methods of materials testing and analysis.
PACS 83.80.Nb – Geological materials: Earth, magma, ice, rocks, etc.

1. – Introduction

Villa Adriana at Tivoli (Rome) is an exceptional complex of classical buildings which is inscribed by the UNESCO in the World Heritage List. It was designed and erected in the 2nd century AD by the Roman Emperor Hadrian. Analytical investigations on the monumental complexes of the Roman Empire Age complement the studies carried out on architectural and building engineering in order to achieve unitary views on this historical period. The present investigation on the microstructures of marble fragments is carried out within the RiVA ("*Rivelare Villa Adriana – Ristudiare Villa Adriana*")

(*) The authors of this paper have agreed to not receive the proofs for correction.

initiative([1]), aiming at a thorough chemical-physical analysis of the large variety of Villa Adriana artistic artefacts, in a multidisciplinary approach. Neutron diffraction has been used in this context for the characterisation of ancient Roman marble fragments from the Palace "Edificio con Tre Esedre", located inside Villa Adriana.

The great majority of monuments, statues and other objects of archaeological interest in the Villa are made of marble. For those objects attribution, provenance and state of conservation are of key importance. At the same time, calcite rocks such as limestone and marble are some of the most studied minerals in Earth sciences. Marble is typically composed of carbonate minerals such as calcite and dolomite, whilst silicates (such as quartz, plagioclase, micas), oxides (such as rutile, magnetite), and phosphates (such as apatite) can be present as trace or minor phases. Natural calcite rocks and marbles commonly exhibit preferred orientation (texture) which forms during growth or deformation and which is modified during re-crystallization and plastic tectonic deformations. The characterisation and measurement of the preferred orientation of grains in rocks is the subject of texture analysis [1]. Marble is an important component in this field because calcite is very suitable for deformation experiments, results of which can be compared to naturally deformed materials [2,3]. The geological textures, formed over millions of years, are not affected by quarrying or stone sculpting. Thus, in the archaeological context, the texture analysis of marble may help in the purpose of attribution and provenance determination. Moreover, it may be of use in the field of conservation: for instance, the weathering of marble by anisotropic thermal expansion is influenced by the crystallographic textures [4].

As far as marble provenance is concerned, from the historical point of view, some Roman marble quarries have been located, but not exactly those that have been used to extract Villa Adriana's marbles. Nevertheless, probably white marbles come from Luni (in the actual Liguria), colored ones from Egypt, Turkey, Greece and some others from North Africa.

In this paper we have present analyses of 25 marble and rock fragments from the Villa Adriana with regard to mineral phase compositions and crystallographic textures. The fragments originate from the "Edificio con Tre Esedre", in particular from a room of the Palace indicated as TE7. The marble samples were part of the wall decoration of the building, for which a reconstruction is shown in fig. 1 [5]. The marble decoration was realized with the *opus sectile* technique, typical of Hadrian's time, therefore the wall decoration belongs to the II century a.C. In this case, for the first time marble fragments of a wall covering have been discovered *in situ*. The fragments analysed in this paper are coming from the first comb rubbing and have been chosen as representative sampling of the discovered marbles.

The fragments would have allowed sampling of a small amount of material to be used for more conventional phase analysis techniques such as X-ray diffraction. However, neutron diffraction is a very suitable technique for texture analysis of geological samples [6]. Due to the low absorption of neutrons in matter, large sample volumes of coarse grain materials (such as rocks) can be easily investigated. Low absorption of the neutrons means high penetration into the interior of the sample (several cm), which is an advantage for investigating geological materials. In the context of archaeological studies it is important to emphasize that the high penetration power of neutrons allows for the

([1]) A joint project involving the University of Rome Tor Vergata and the Italian Ministry of Cultural Heritage – *"Soprintendenza per i Beni Archeologici del Lazio"*.

Fig. 1. – Reconstruction of the marble wall decoration of the Palace "Edificio con Tre Esedre". The examined marble fragments were part of this decoration [4A].

non-invasive analysis of an intact, unique object. Average structural information can be derived from a large sample volume of an undisturbed object [7], hence results are very likely representative for the whole object.

The characterisation of historic objects and archaeological findings by neutron diffraction (structure analysis) well complements other established neutron-based diagnostic techniques such as neutron activation analysis (elemental composition) and neutron tomography (visualization of internal features). In this paper we take the marble study as an example and present some latest developments of neutron diffraction analyses of cultural heritage materials [8, 9]. Recent developments of neutron instruments and of data analysis techniques opened the prospects for rapid non-destructive, quantitative structure and texture analyses of intact unique museum objects. One of the first neutron texture analyses on Cultural Heritage objects has been performed on the Early Copper Age Iceman axe [10]. Texture analysis with time-of-flight neutron diffraction (TOF-ND) at accelerator based spallation sources is currently being established but it has already shown its potential as innovative technique in geological and archaeological sciences. Examples are studies on poly-mineralic rocks [11], historic silver coins [12, 13], as well as bronzes objects [14, 15].

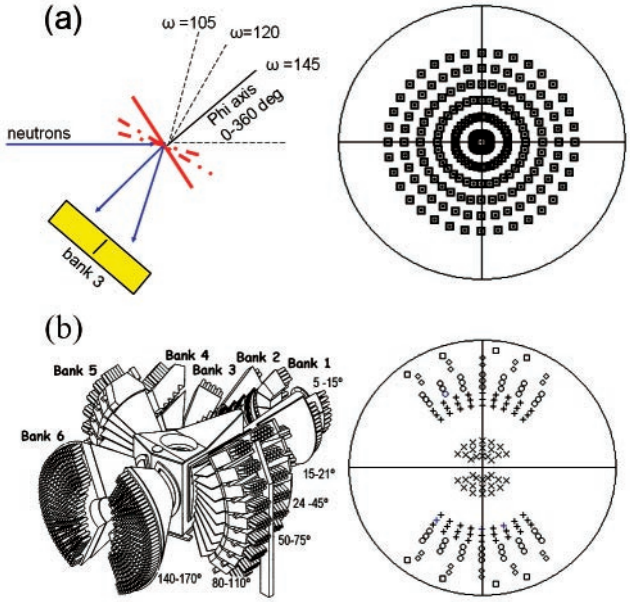

Fig. 2. – ROTAX (a) and GEM (b) instrument schematics, pole figure coverages for texture measurements (see text).

2. – Experimental

2˙1. *Methodical background on TOF texture analysis.* – For archaeological samples that are usually multi-phase, diffraction analysis (by X-rays, electrons, neutrons) provides quantitative information on one or more of the following structural levels: i) phase composition, ii) crystal structure of each phase, iii) "grain structure" that represents sizes, shapes and mutual orientations (texture) of grains, and iv) microstructure describing structural deviations from an ideal crystal within grains [16]. With neutron diffraction a full structural characterisation can be achieved on the objects without sampling, special preparation or cleaning. The use of time-of-flight (TOF) techniques allows a rapid acquisition of data on stationary archaeological objects [17-19], the main advantage being that complete diffraction patterns can be collected in backscattering angles. A further benefit of texture analysis on TOF instruments is the simultaneous measurement of many pole figures (corresponding to many Bragg peaks) for all the phases present in the sample.

The presence of texture manifests itself as intensity variations of Bragg peak as a function of the detector angle. Texture of a material is conveniently displayed by its pole figures which are measured by recording diffraction patterns as a function of the scattering angle, either by i) rotating the sample on a goniometer and/or by ii) using a multi-detector surrounding the sample. The first option is the conventional texture scanning set-up and is adopted on ROTAX [17,18] whereas the second option is realized on GEM [20] both being operated as neutron TOF diffractometers at the ISIS spallation source at the Rutherford Appleton Laboratory, UK. Figure 2 shows the scanning schematics and corresponding pole figure coverages for these two instruments.

By using a polychromatic beam and with many detectors at fixed scattering angles

like on GEM, TOF neutron diffraction has some considerable advantages for texture analysis since significant portions of both reciprocal space and orientation space are simultaneously covered in one measurement. The capabilities and benefits of extracting the orientation distribution function (ODF) of a material from TOF data is well documented both from the experimental and the data treatment point of view. TOF texture analysis with a multidetector set-up was previously demonstrated at the pulsed source IBR-2, Russia [21] and at the pulsed spallation source LANSCE, USA [22]. Moreover, in the past few years Rietveld codes such as GSAS [23] and MAUD [24, 25] have been developed to determine texture coefficients from TOF data. By increasing the detector coverage on a TOF diffractometer fewer sample rotations are required for quantitative texture analysis, as it was demonstrated on HIPPO at LANCSE [22, 26] with typically 4-8 sample orientations and total collection times in the order of 20 minutes. Here we show that on GEM at ISIS, quantitative texture information can be obtained even faster from a single measurement without any sample reorientations. Results on calcite and marble samples measured on TOF instruments with small (ROTAX) and large (GEM) detector coverage are compared.

ROTAX has three linear position-sensitive scintillation detectors installed in the horizontal diffraction plane. For the texture measurements only one of those detectors, installed at backscattering angle ($2\Theta = 120°$), was used because its view is unobstructed by the goniometer and because the best resolution is achieved at backscattering angles. The scintillator (75 mm heigh, covering a vertical angle of 3.8° at a distance of 1.125 m) covers approximately $2\Theta = 40°$ in scattering angle, as indicated in fig. 2a. For the sample orientation on ROTAX a two-axis goniometer is used, with goniometer angles ω about the vertical diffractometer axis and φ about the horizontal sample axis (fig. 2a, left). The "zero position" ($\omega = \varphi = 0$) has the φ-axis pointing along the outgoing primary neutron beam direction. The pole figure coverage (fig. 2a, right) and the pole figure angles (α = pole distance angle, β = azimuth angle) are functions of the goniometer angles and the detector position: $\alpha = 90 + \Theta - \omega$, $\beta = \varphi$. For three ω-setting (145°, 120°, 105°) the sample was rotated about the horizontal φ-axis by 360° (in 10° steps); since the detector has been split by software into two parts, one obtains $36 \times 3 \times 2 = 216$ orientation points in the pole figure. In other words, for a certain ω-setting, varying φ describe *two* small-circles in the pole figure. For small samples from the Villa Adriana a further ω-setting of 85° was used to cover the outer regions of the pole figure (not shown in fig. 2a) corresponding to 288 orientation points.

GEM is equipped with 6 detector banks, housing a total of about 7000 individual detector elements arranged as schematically shown in fig. 2b. Each detector element provides a TOF diffraction pattern and "views" the sample from a different direction. One detector element is typically about $5 \times 200\,\mathrm{mm}^2$ in size, corresponding to an angular coverage of about $0.2 \times 10\,\mathrm{deg}^2$ for a typical sample-detector distance at $2\Theta = 90°$. The total detector coverage of GEM exceeds 4 sterads, hence providing a considerable coverage in orientation space. For the texture analysis 164 separate detector groups were generated, with each group covering approximately $10 \times 10\,\mathrm{deg}^2$. The corresponding pole figure coverage for a single sample orientation (the "zero position") is shown in fig. 2b (right), with the backscattering bank-6 detector groups in the pole figure centre. It has to be kept in mind that a symbol in the pole figure in fig. 2b represents the angular location of a group of detectors. Hence one group records a range of sample orientations over which intensities are averaged, thus affecting the achievable angular texture resolution. The unique advantage of GEM for texture analysis is that the sample does not need to be rotated. As a consequence, texture of complex objects can be obtained in a rapid

single shot in a stationary set-up.

The three-dimensional orientation distribution function (ODF) can be derived from pole figures with various mathematical procedures [26,27]. Since TOF neutron diffraction simultaneously records a large number of Bragg peaks, *i.e.* pole figures, whole patterns fitting methods are very efficient to extract the texture information directly from the set of TOF diffraction spectra via full pattern profile fitting algorithms. The data are, for each single pattern, normalized to the incident neutron flux distribution, corrected for detector efficiencies, and converted into 216 and 164 d-spacing patterns for ROTAX and GEM respectively, corresponding to pole figures coverages in fig. 2a, b. We have used the E-WIMV (Extended-WIMV) algorithm [24, 26] to extract values of the ODF cells as implemented in the MAUD program [25]. E-WIMV can handle incomplete and highly irregular pole figure coverages, as the one shown in fig. 2b. Application of the E-WIMV algorithm has been previously discussed in detail [22, 24, 26]. In order to account for sample absorption anisotropy due to the sample shape, one scale factors for each diffraction pattern was refined. Pole figures are reconstructed with MAUD from the ODF and are shown in equal area projection in this paper.

2˙2. *Collection of marble pole figures at ISIS.* – Neutron diffraction data on 25 marble samples (dimensions: 2–6 × 1–3 cm, about 5 mm thickness) from Villa Adriana were collected on ROTAX (22 samples) and GEM (3 samples). The beam size for both instruments was 20 × 20 mm. Each sample, placed inside a vanadium pocket, was positioned inside an evacuated sample-chamber. The collection times were 1 hour on ROTAX and 20 minutes on GEM. The data collected on such a stationary sample were analysed with the Rietveld method using the GSAS program [23], using all available diffraction histograms (3 on ROTAX and 6 GEM). The analysis yielded the phase fraction of the identified phases and lattice parameters of the calcite phase.

The patterns collected on GEM on the fixed sample were also used for extracting the texture information, taking into account that the marble slabs were mounted with the incoming neutron beam normal to the slab surface.

For 8 samples (out of the 22 marble fragments measured on ROTAX), also texture data were recorded on ROTAX. Each sample, taped to an aluminium sample-holder, was mounted onto a two-axis goniometer, installed inside the evacuated sample chamber. The sample was rotated into 108 or 144 different orientations (each measured for 2 minutes) in order to produce the diffraction pattern used to reconstruct the pole figures. A scaling was applied to the individual raw spectra in order to account for the change of the illuminated sample volume of the plate-shaped fragments for different ω-settings. The pole figures were calculated with the program MAUD [25]. The total counting time was about 5 hours for 108 sample orientations. For small marble fragments an extra $\omega = 85°$ setting was used, but not for bigger slabs (*e.g.*, n. 22) because this ω position corresponds to an almost grazing incidence of the neutron beam, resulting in strongly distorted peak profiles.

3. – Results and discussion

3˙1. *TOF neutron texture analysis on ROTAX and GEM.* – TOF texture analysis benefits from the simultaneous coverage of *d*-spacing range, *i.e.* number of pole figures, and of scattering angles. For ROTAX data we used the backscattering bank and a regular scanning grid where each orientation point has approximately the same statistical weight in the ODF calculation. For GEM, the forward-scattering banks are less effective in the

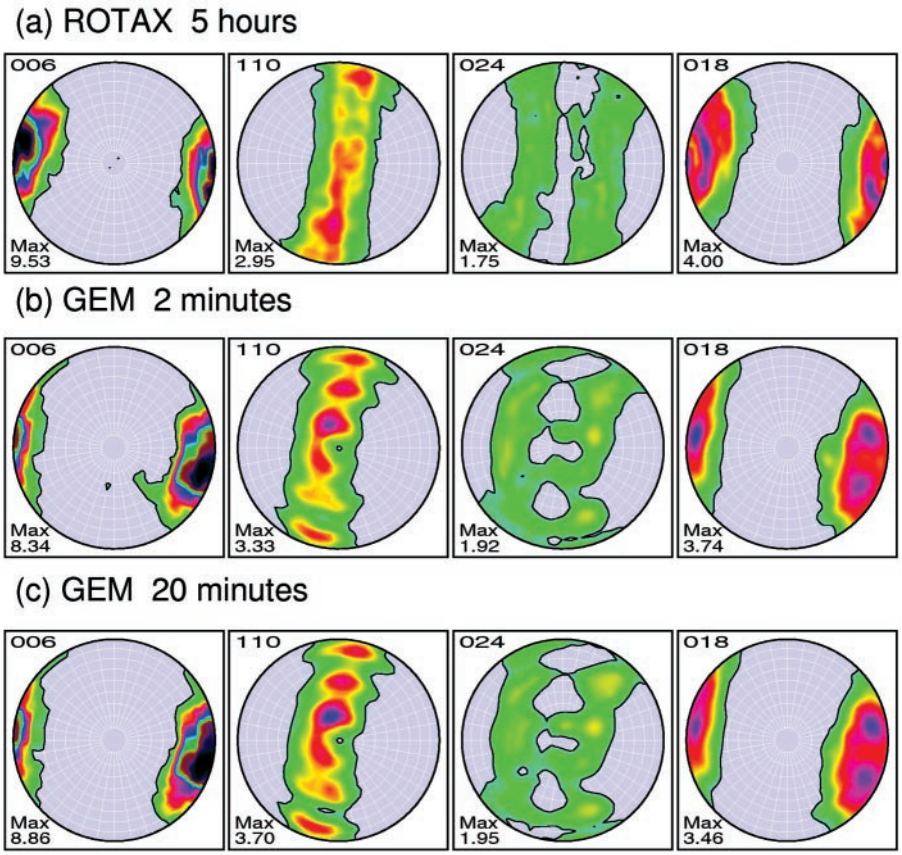

Fig. 3. – Reconstructed calcite pole figure of a reference specimen from ROTAX data (a) and GEM data (b, c).

quantitative texture analysis than the high-angle banks, due to the smaller number of Bragg peaks observed in the former. Pole figures of a reference calcite sample measured both on ROTAX and GEM are reported in fig. 3. For the calcite pole figures, the denotation of planes (006), (110), (024) and (018) follows the short form of Bragg indices of the trigonal calcite crystal system, *e.g.* (006) and (110) stand for (0006) and (11-20), respectively. The (006) pole figure represents the *c*-axis distribution. The (110) pole figure is representative of the *a*-axis distribution. The maximum *m.r.d.*-values (*m.r.d.*: multiples of a random distribution) are given in fig. 3 to represent the strength of a texture. Pole figures are in the following represented in equal area projection and, for reasons of clarity, pole densities are plotted only for *m.r.d.* greater than one. The pole figures collected on ROTAX and GEM are in overall agreement. There are noticeable although acceptable differences in maximum *m.r.d.* values for one and the same (hkl). It is important to note that the main features of the texture in terms of symmetry and texture strength are achieved after a collection time of 2 minutes on GEM, compared to 5 hours on ROTAX. It is a major result of this study that texture information can be obtained in a matter of minutes on a stationary sample.

TABLE I. – *Identified mineral phases and mineral weight fractions of marble samples from the Villa Adriana. The weight fractions for illite-muscovite can be considered only as rough estimates since no reliable structure model is available. Q /C denotes the ratio quartz over calcite, and I / C the ratio illite over calcite. The Rietveld estimated standard deviation (e.s.d.) of the lattice parameters is about* 0.01%. *The "true" error is considerable higher, in the order* 0.005 *Å for the a-lattice constant and* 0.02 *Å for the c-lattice parameter, as obtained from repeated collections on one and the same sample. The systematic error on the phase fractions is of the order of* 0.2 *wt%. For the texture analysis the maximum m.r.d. (multiples of a random distribution) values for the* (006) *pole figures, representing the c-axis distribution, are also reported to represent the texture strength.*

Sample n.	Calcite latt. param.		Phase							Texture
	a (=b) (Å)	c (Å)	Calcite (%)	Quartz (%)	Dolomite (%)	Illite (%)	Plagioclase (%)	Q/C (%)	I/C (%)	max. m.r.d. (006)
Type A										
2	4.996	17.08	100	0	0	0	0	0	0	
17	4.985	16.98	100	0	0	0	0	0	0	13.8
18	4.993	17.07	100	0	0	0	0	0	0	1.78
22	4.994	17.07	100	0	0	0	0	0	0	1.42
25	4.995	17.07	100	0	0	0	0	0	0	
29	4.989	17.05	100	0	0	0	0	0	0	
30	5.003	17.10	100	0	0	0	0	0	0	13.8
8b	4.990	17.06	100	0	0	0	0	0	0	3.62
Type B										
1	4.994	17.07	79.13	0.24	0.73	20.86	0	0.3	26.4	
3	4.987	17.04	89.81	0.70	0.31	9.18	0	0.8	10.2	1.64
5	4.992	17.07	89.11	1.02	0.82	9.86	0	1.1	11.1	
9	4.987	17.04	85.14	1.85	0.78	12.99	0	2.2	15.3	1.57
28	4.989	17.05	78.17	2.55	0.72	19.27	0	3.3	24.7	1.28
31	4.990	17.06	87.14	1.93	0.80	10.92	0	2.2	12.5	
33	4.992	17.06	80.88	0.42	0.74	16.26	2.42	0.5	20.1	
Type C										
11	4.977	17.01	82.83	16.19	0.97	0	0	19.5	0	1.22
16	4.977	17.01	83.32	14.79	1.90	0	0	17.7	0	1.17
21	4.978	17.01	85.23	14.74	0.02	0	0	17.3	0	

3˙2. *Phase analysis.* – The results of the Rietveld refinement performed with the GSAS program are reported in table I. For each examined sample the identified mineral phases and mineral weight fractions are reported: calcite [$CaCO_3$], quartz [SiO_2], dolomite [$CaMg(CO_3)_2$], illite-muscovite [$K_yAl_4(Si_{8-y}, Al_y)O_{20}(OH)_4$], plagioclase [$(Ca, Na)Al_2Si_2O_8$] are the identified and quantified phases. The refined lattice parameters for the calcite phase are also given. For each identified phase, a weight fraction can be attributed, apart for the phase indicated as illite-muscovite, for which a reliable structure model is not available. For this mineral we can just give rough estimates of its presence in the sample. Following the presence of quartz and illite with respect to calcite, the marbles have been classified into 4 categories: Type-A samples consist practically of pure calcite. Type-B samples contain between 80 to 90 wt% calcite, whilst illite-muscovite is present in relevant quantities and the relative weight of

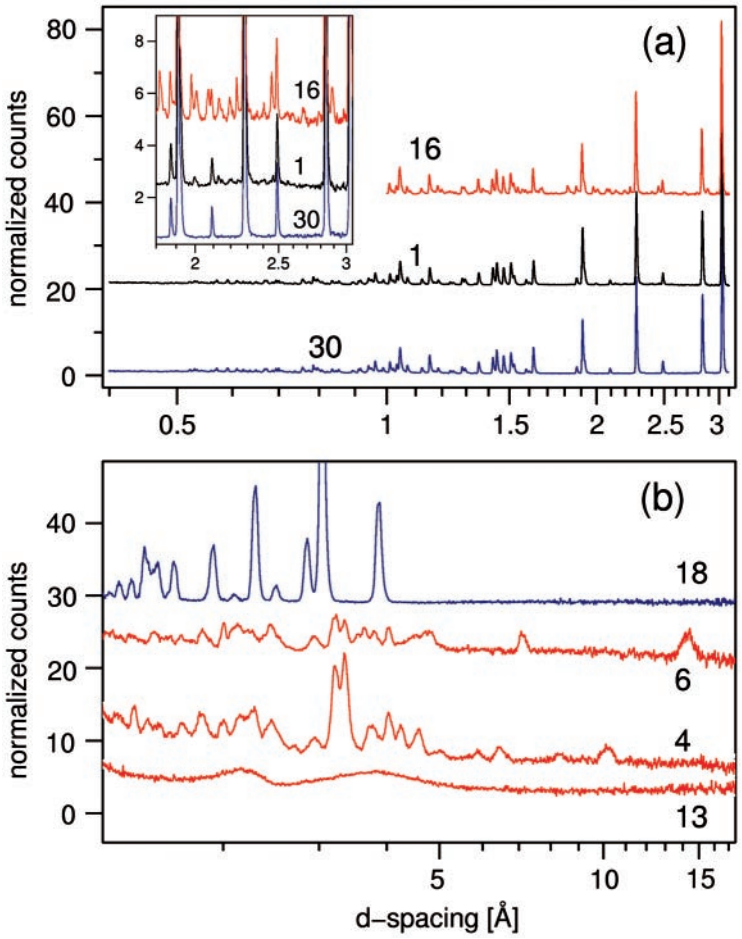

Fig. 4. – Neutron diffraction patterns of marble fragments: (a) Type A (bottom, 30, pure calcite), Type B (middle, 1, mainly calcite + illite-muscovite), and Type C (top, 16, mainly calcite + quartz). The insert highlights the Bragg peaks of the minority phases. (b) Patterns from Type D samples from Villa Adriana, with no or low calcite content, compared to a Type-A marble fragment. From top to bottom: 18 (pure calcite); 6 (mainly chloride, feldspars, quartz); 4 (mainly illite-muscovite, feldspars, quartz); 13 (silica glass).

quartz is between 0.3 and 3.3%. Type C contains samples that exhibit calcite around 84 wt% of the total whereas the rest is quartz amounting to about 15 wt%. A fourth group (Type D, not shown in table I, samples n. 20, 4, 6, 5b) does have a low or no calcite but mainly plagioclase and quartz plus smaller and varying fractions of chlorite, sericite, illite-muscovite and probably hornblende. One sample (n.13) in that group is a glass sample. One of the samples in category D (n. 5b) consists of 99.4 wt% dolomite and 0.6 wt% calcite.

Figure 4 compares observed neutron diffraction patterns of some of the marble fragments of the different groups A-D. Figure 5 shows profile fitted diffraction patterns for marble fragment n. 11 (Type C). The mineral phase fractions of Type D were not quanti-

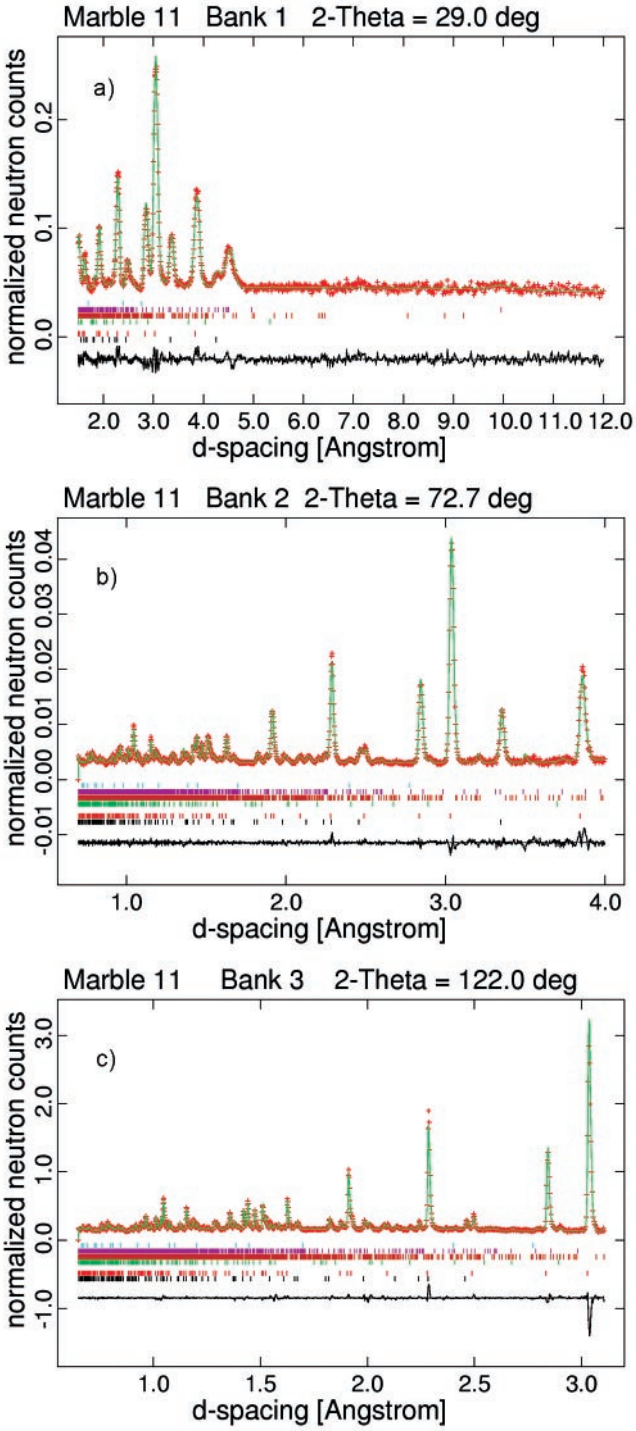

Fig. 5. – Measured data (symbols), calculated patterns (solid line), and difference between the observed and calculated intensities (lower curve) of marble fragment n. 11. The bar codes indicate the theoretical peak positions of the different phases (bottom to top): quartz, calcite, illite, dolomite, plagioclase, muscovite, lime. The three patterns correspond to the three detector units on ROTAX.

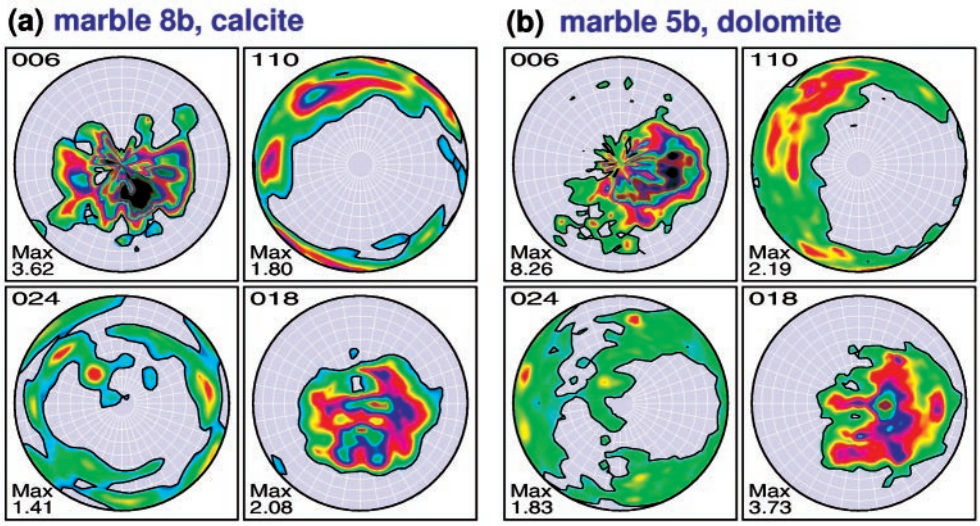

Fig. 6. – Pole figures (006, 110, 024, 018) of marble sample 8b (calcite) and 5b (dolomite), from data measured on GEM.

fied because of the uncertain hydrogen positions for some of the crystal structure models. That is to say, reliable structure models are required for determining accurate phase fractions with the Rietveld method. In case all structures are known, the Rietveld analysis is a robust method for quantitative phase analysis powerful when internal standards cannot be used, *e.g.*, for intact archaeological artefacts. The quantitative assessment is hampered if some of the crystal structures of the constituent phases are not fully solved, *e.g.* in the case of unknown hydrogen positions of clay minerals.

For type-C samples the lattice parameters resulting from the refinements of calcite are systematically reduced, whereas for type-A and type-B sample the calcite unit cell adopts the expected values. The amount of the reduction for type-C sample agrees with a substitution of Ca by Mg in the order of about 4 mol%.

In conclusion, the phase analysis performed on the Villa Adriana marble fragments allows for a clear separation into four different groups.

3˙3. *Texture analysis*. – Pole figures collected from several marble fragments indicate more or less pronounced deviations from a random crystallite orientation distribution. Figure 6 compares calcite and dolomite pole figures collected on GEM on samples 8b and 5b, respectively. Figure 7 shows representative pole figures produced from (006), (110), (024) and (018) Bragg peaks, for 4 of the samples (n. 16, 17, 18, 28). The projection plane of the pole figure is always parallel to the largest surface of a sample. For example, the strong maxima in the (006) pole figure of sample 18 in fig. 7 indicate a preferred alignment of the crystallographic calcite *c*-axis parallel to the sample surface. Figure 8 compares the (006) pole figures for eight samples from the Villa Adriana (n. 3, 9, 11, 16, 17, 18, 22, 28) with the calcite geological reference sample from Syros.

Whereas the dolomite sample (fig. 6b) exhibits a rather strong texture (texture index 5.7), all the calcite textures are comparatively weak with texture indices between 1 and 2, except for n. 17. Four samples (3, 18, 22, 8b) exhibit characteristic and strong (006) pole density maxima that are complemented by density girdles along perpendicular directions

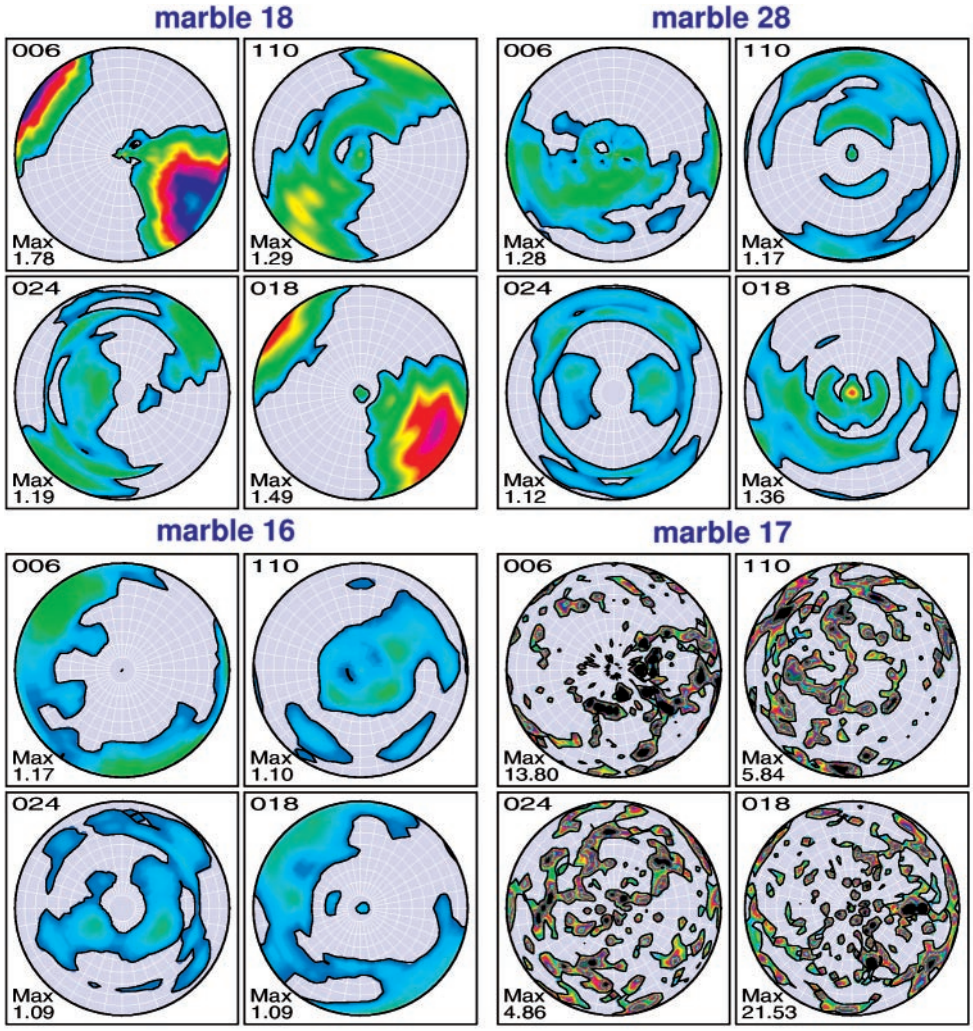

Fig. 7. – Pole figures (006, 110, 024, 018) of four marble fragments (n. 16, 17, 18, 28), each of them representing a different texture type.

in the (110) pole figures. The maximal *m.r.d.* values vary between 1.4 and 1.8. For a second group of samples (9, 11, 28) the (006) density maxima are less pronounced, but rather distributed over several maxima or over a girdle of pole density. Marble fragment 16 represents a very weak type of texture with a maximum of less than 1.2 *m.r.d.* from a random distribution. It should be noted that the distinction between sample 16 and the second group in terms of texture type and texture strength is rather difficult and arbitrary. Sample 17 shows a totally different distribution with sharp and randomly distributed pole density maxima, unlike a typical marble sample and rather typical for a coarse-grain material with a rather small number of large calcite crystallites. The reference sample displays a strong texture (max. *m.r.d.* 7) with the same type of texture as for 3, 18, and 22 and 8b.

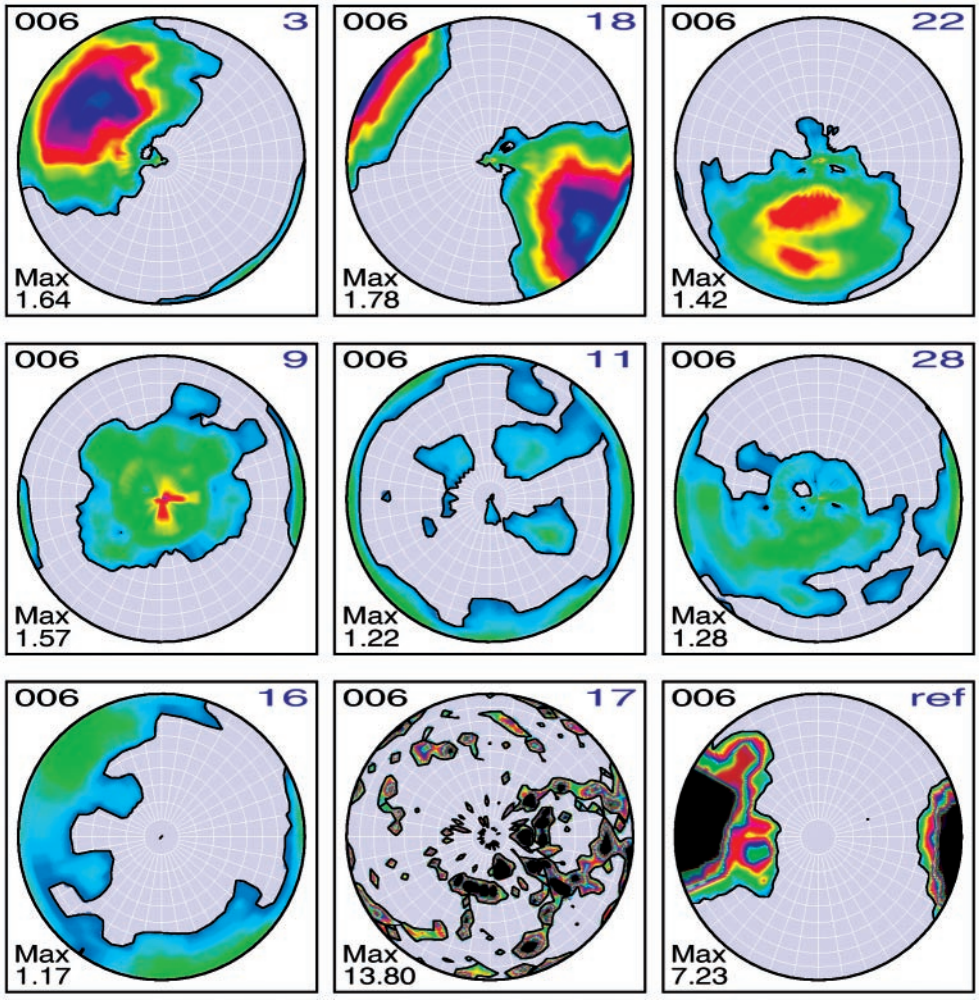

Fig. 8. – Maps of the *c*-axis distributions, represented by the (006) pole figures, of marble samples from the Villa Adriana, compared to a geological calcite reference sample from Syros, Greece. The marble and reference (ref) samples have been measured on ROTAX and GEM, respectively. For each (006) pole figure, the maximum *m.r.d.* is given.

The fragments thus can be distinguished by their distinct crystallographic preferred orientations which are caused by different geological deformation processes. Comparing our results with that of the reference sample and with those from the literature [1,2], the textures of marble fragments 3, 18, 22, and 8b are quite typical for natural calcites that have suffered "pure shear" or "simple shear" deformations [1]. Pure shear corresponds to uniaxial flattening of the calcite rock, which aligns the *c*-axes (the (006) poles) along the compression direction (orthorhombic texture symmetry). Simple-shear corresponds to a shearing of the calcite rock, with the *c*-axis maximum inclined against the direction of shear (monoclinic texture symmetry). For pure shear, (006) pole maxima are produced normal to the shear/flattening plane. For simple shear, (006) pole maxima are inclined

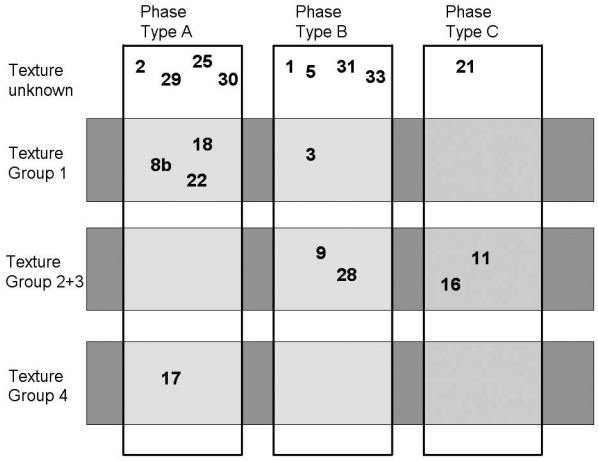

Fig. 9. – Correlation plot of maximum pole density (*m.r.d.*) of (006) pole figure *vs.* phase fraction ratio Q / C (quartz / calcite) and I / C (illite / calcite). The number of the sample is used as a symbol in the plot. There is a tendency of the strong textured samples (Texture Group 1) to belong to phase groups A-B whereas the weak textures (Texture Group 2 and 3) belong to phase groups B-C.

to the normal of the shear plane. The angle of inclination can, in geoscientific studies, be used to determine the type of deformation and the ratio between simple and pure shear. However for archaeological marble objects, the geological setting and the reference system are usually not obvious and known, *e.g.*, how the sample was removed from the geological rock formation. The foliation planes and lineation directions are not evident for samples which cannot be cut, polished or broken. Hence, the texture symmetry cannot be obtained. For the weaker textures of marble 28 and 16, the deformation process must have been more complicated.

It can be concluded that distinct textures types are observed for Villa Adriana marble samples. Samples that exhibit the same texture type do not necessarily belong to the same phase groups A-D as given in table I, as is evident in fig. 9. The figure separates the marble samples into phase and texture group according the phase types in table I and to the texture strength and texture type as discussed above. The sample groups (n. 18, 22, 8b), (n. 9, 28), and (11, 16) are strongly related, respectively, in terms of characterisation attributes like phase, structure and crystallographic texture.

4. – Conclusions

Neutron radiation is a versatile diagnostic probe for collecting essential information from the interior of large, undisturbed archaeological materials and objects of art. Neutrons penetrate through coatings and corrosion layers deep into centimetre-thick artefacts without substantial attenuation. This property makes them ideal for non-destructive testing of unique and precious objects for which sampling are unacceptable. A particular attraction of neutron techniques for archaeologists and conservation scientists is the prospect of locating hidden materials and structures inside artefacts. Samples can be measured as they are, without cleaning and mechanical polishing.

We have studied archaeological marble for which the geological setting is *a priori*

unknown. Texture maps together with phase analysis can differentiate between different types of marble. Our study shows for the first time that the pole figures can be obtained in a very short time as little as 2 minutes on a TOF neutron diffractometer. Rapid measurements of textures are of interest for measuring large sample series or for analysing bulky objects that cannot be oriented on a gonimeter. For archaeological samples, it is beneficial to keep neutron irradiation to a minimum for reducing the activation decay times, and hence the storage requirements at the neutron facilities. This is particularly important for some metals like copper and silver while for the marble samples of this study the induced activation decayed after a few minutes.

Although the present study used marble fragments, it should be underlined that neutron diffraction could as well be carried out on intact objects of almost any shape such as vessels and figurines. This is an important prospect for objects, for which coring, cutting, or cleaning is unacceptable. We believe that any structural features, and in particular the crystallographic texture, of a marble object could be useful attribution characteristics. Whether or not the texture can be used for provenance purposes remains to be further explored with a larger selection of marble samples, in particular with reference samples from certified sources and quarries. Certainly a useful application is in the field of marble restoration. A previous intervention on an object could be easily identified and the original part well distinguished from an added one, in a non-invasive way, using the phase composition, the type and strengths of textures and the preferred orientation directions with respect to the shape of the object as indicators.

* * *

The authors acknowledge Dr. B. Adembri, Director of Villa Adriana, from the *"Soprintendenza per i Beni Archeologici del Lazio"* of the Italian Ministry of Cultural Heritage, for making the samples available and Prof. G. E. Cinque, coordinator of the RiVA Project, supporter of the present investigation. We thank Prof. R. Triolo, University of Palermo, Italy, and J. Walter, Forschungszentrum Jülich, Germany, for the valuable discussions and C. M. Goodway and D. Cowdery for their technical support during the experiments. Support by L. Lutterotti, University of Trento, Italy, with the MAUD program is gratefully acknowledged. This work was supported within the CNR-CCLRC Agreement No. 01/9001 concerning collaboration in scientific research at the spallation neutron source ISIS. The financial support of the Consiglio Nazionale delle Ricerche in this research is hereby acknowledged.

REFERENCES

[1] Wenk H.-R and Van Houtte P., *Rep. Prog. Phys.*, **67** (2004) 1367.
[2] Leiss B. and Molli G., *J. Struct. Geol.*, **25** (2003) 649.
[3] Barnhorn A., Bystricky M., Burlini L. and Kunze K., *J. Struct. Geol.*, **26** (2004) 885.
[4] Siegesmund S., Ullemeyer K., Weiss T. and Tschegg E. K., *Int. J. Earth Sci.*, **89** (2000) 170.
[5] Cinque G. E., *Ricostruzione della decorazione parietale di un ambiente dell'Edificio con Tre Esedre di Villa Adriana*, in *A Tivoli Vecchio, a Casa di Adriano* (Gangemi, Roma) 2005.
[6] Schäfer W., *Eur. J. Mineralogy*, **14** (2002) 263.
[7] Kockelmann W., Kirfel A. and Hähnel E., *J. Archaeol. Sci.*, **28** (2001) 213.
[8] Rinaldi R., Artioli G., Kockelmann W., Kirfel A. and Siano S., *Notiziario Neutroni e Luce di Sincrotrone*, **7** (2002) 30.

[9] Siano S., Kockelmann W., Bafile U., Celli M., Iozzo M., Miccio M., Moze O., Pini R., Salimbeni R. and Zoppi M., *Appl. Phys. A*, **74** (2002) S1139.
[10] Artioli G., Dugnani M., Hansen T., Lutterotti L., Pedrotti A. and Sperl G., in *La mummia dell'età del rame. 2. Nuove ricerche sull'uomo venuto dal ghiaccio*, edited by Fleckinger A., Vol. **3** (Folio Verlag, Bolzano) 2003, p. 9.
[11] Wenk H.-R., Cont L., Lutterotti L., Ratschbacher L. and Richardson J., *J. Appl. Cryst.*, **34** (2001) 442.
[12] Kockelmann W., Kirfel A., Jansen E., Linke R., Schreiner M., Traum R. and Denk R., in *Proc. Numismatics & Technology, Kunsthistorisches Museum Wien*, 2003, p. 113.
[13] Yanxia Xie, Lutterotti L., Wenk H.-R. and Kovacs F., *J. Mater. Sci.*, **39** (2004) 3329.
[14] Siano S., Bartoli L., Kockelmann W., Zoppi M. and Miccio M., *Physica B*, **350** (2004) 123.
[15] Pantos E., Kockelmann W., Chapon L. C., Lutterotti L., Bennet S. L., Tobin M. J., Mosselmans J. F. W., Pradell T., Salvado N., Buty S., Garner R. and Prag A. J. N. W., *Nucl Instrum. Methods B, Phys. Res. B*, **239** (2005) 16.
[16] Bunge H. J., *Texture and structure of polycrystals*, in *Defect and Microstructure Analysis by Diffraction*, edited by Snyder R. L., Fiala J. and Bunge H. J. (International Union of Crystallography, Oxford University Press) 1999, p. 405.
[17] Kockelmann W. and Kirfel A., *Physica B*, **350** (2004) e581.
[18] Kockelmann W., Pantos E. and Kirfel A., in *Radiation in Art and Archeometry*, edited by Creagh D. C. and Bradley D. A. (Elsevier ISBN 0-444-50487-7) 2000, p. 347.
[19] Siano S., Bartoli L., Zoppi M., Kockelmann W., Daymond M., Dann J. A., Garagnani M. G. and Miccio M., in *Europe 2, Proc. Archaeometallurgy*, 2003, p. 319.
[20] Day P., Enderby J. E., Williams W. G., Chapon L. C., Hannon A. C., Radaelli P. G. and Soper A. K., *Neutron News*, **15** (2004) 19.
[21] Feldmann K., Betzl M., Kleinsteuber M. and Walther K., *Textures and Microstructures*, **114** (1991) 59.
[22] Wenk H.-R., Lutterotti L. and Vogel S., *Nucl. Instrum. Methods A*, **515** (2003) 575.
[23] Von Dreele R. B., *J. Appl. Cryst.*, **30** (1997) 517.
[24] Lutterotti L., Matthies S., Wenk H.-R., Schultz A. S. and Richardson jr. J. W., *J. Appl. Phys.*, **81** (1997) 594.
[25] Lutterotti L., *MAUD, Material Analysis using Diffraction* (www.ing.unitn.it/∼luttero/maud/index.html)
[26] Matthies S., Pehl J., Wenk H.-R., Lutterotti L. and Vogel S. C., *J. Appl. Cryst.*, **38** (2005) 462.
[27] Kocks U. F., Tomé C. N. and Wenk H.-R., in *Texture and Anisotropy* (Cambridge University Press) 1998.